

Directing the crystal packing in triphenylphosphine gold(I) thiolates by ligand fluorination

Guillermo Moreno-Alcántar,^{§,} Luis Turcio García,[§] José M. Guevara-Vela,[‡] Eduardo Romero-Montalvo,[‡] Tomás Rocha-Rinza,[‡] Ángel Martín Pendás,[†] Marcos Flores-Álamo[§] and Hugo Torrens[§]*

[§]School of Chemistry, National Autonomous University of Mexico, Circuito Escolar, Ciudad Universitaria, Coyoacán, 04510 Mexico City, Mexico.

[†]Institut de Science et d' Ingénierie Supramoléculaires (ISIS), University of Strasbourg. 8 allée Gaspard Monge, 67000, Strasbourg, France. *E-mail: morenoalcantar@unistra.fr

[‡]Institute of Chemistry, National Autonomous University of Mexico, Circuito Exterior, Ciudad Universitaria, Coyoacán, 04510, Mexico City, Mexico.

[†]Department of Analytical and Physical Chemistry, University of Oviedo, E-33006, Julián Clavería, 8, 33006, Oviedo, Spain.

KEYWORDS. Supramolecular chemistry, gold, aurophilic interactions, fluorothiolate, QTAIM, NCI-index.

ABSTRACT

We explore herein the supramolecular interactions that control the crystalline packing in a series of fluorothiolate triphenylphosphine gold(I) compounds with the general formula $[\text{Au}(\text{SR}_F)(\text{Ph}_3\text{P})]$ in which Ph_3P = triphenylphosphine and $\text{SR}_F = \text{SC}_6\text{F}_5$, SC_6HF_4 -4, $\text{SC}_6\text{F}_4(\text{CF}_3)$ -4, $\text{SC}_6\text{H}_3\text{F}_2$ -2,4, $\text{SC}_6\text{H}_3\text{F}_2$ -3,4, $\text{SC}_6\text{H}_3\text{F}_2$ -3,5, $\text{SC}_6\text{H}_4(\text{CF}_3)$ -2, $\text{SC}_6\text{H}_4\text{F}$ -2, $\text{SC}_6\text{H}_4\text{F}$ -3, $\text{SC}_6\text{H}_4\text{F}$ -4, SCF_3 and SCH_2CF_3 . We use for this purpose (i) DFT electronic structure calculations and (ii) the Quantum Theory of Atoms in Molecules and the Non-Covalent Interactions index methods of wavefunction analyses. Our combined experimental and computational approach yields a general understanding of the effects of ligand fluorination in the crystalline self-assembly of the examined systems, in particular, about the relative force of aurophilic contacts compared with other supramolecular interactions. We expect this information to be useful in the design of materials based on gold coordination compounds.

INTRODUCTION

The development of supramolecular chemistry has led to the creation of complex architectures stabilized by weak interactions among organic and inorganic molecules.¹ The fascinating assemblies displayed by inorganic compounds in the solid state are often responsible for desirable physical (optical, magnetic and mechanical)²⁻⁴ as well as chemical properties (gas storage and separation as well as catalysis).^{5,6} Synthetic chemists and crystal engineers strive for the rational control of these properties. Nevertheless, without fully understanding the forces that underlie crystal packaging, these efforts might be futile. The probability that a compound displays any of these desired properties rely on favoring of a given assembly of building blocks over other possibilities. This favoring crucially depends on understanding the relative formation energies of

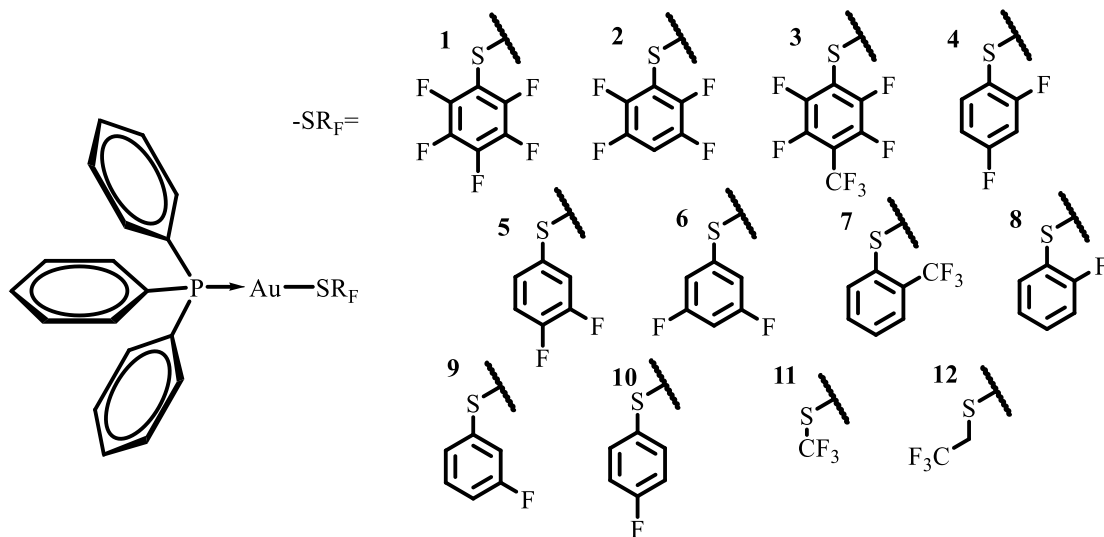
competing aggregates.^{7,8} The strategies aimed to build a predetermined assembly are frequently based on the qualitative and, in some cases, intuitive examination of extensive experimental evidence.^{9,10} However, the experimental quantitative analyses of the relative strength of intermolecular interactions is complicated. For instance, observations are repeatedly non-transferable from one system to others. Therefore, the use of theoretical tools to complement the experimental analysis of non-covalent interactions has been a common and usually successfully alternative in systems containing representative elements.¹¹⁻¹³ Nevertheless, the inclusion of heavy atoms and the intricacy of supramolecular assemblies, particularly for inorganic systems, requires the use of expensive computational methods to get accurate energetic insights.¹⁴⁻¹⁷ In these cases, the exploitation of other theoretical options to the quantitative analysis of supramolecular interactions in inorganic compounds, such as wavefunction analyses, might be valuable.

Concerning the non-covalent interactions which involve gold atoms, Au(I) compounds show an interesting tendency to form short Au \cdots Au contacts, especially in the solid state.¹⁸⁻²⁰ The existence of these contacts is often related to interesting properties of gold-based materials.²¹⁻²⁸ Theoretical studies suggest that these contacts, widely known as aurophilic interactions, result from dispersion interactions and therefore from electron correlation ultimately.^{18,20,29,30,31} Nonetheless, there is also evidence which indicates that the covalent character of Au \cdots Au interactions is important.³²⁻³⁴ The molecular tectonics of gold(I) linear compounds is frequently directed by such gold-gold contacts.³⁵⁻³⁷ However, the occurrence of competing interactions promoted by the structure of the ligands can impair aurophilicity.⁷ Then, the modification of the backbones of the ligands attached to gold atoms is a feasible strategy to tune the interactions which direct the formation of supramolecular architectures. Such modifications can be exploited in the control of aurophilic aggregates.³⁶ For example, electron-withdrawing substituents which decrease the electron density

of Au centers weaken the gold-gold contacts.³⁸ The study of systems wherein the Au \cdots Au interactions are disfavored or overwhelmed by other synthons could underestimate the real significance of these interactions.³⁹ In contrast, the analyses of systems in which the Au \cdots Au contacts are favored indicate that they are as strong as other archetypical supramolecular interactions such as π -stacking and hydrogen bonds.^{37,40} Concerning the characterization of aurophilic contacts, we have already used descriptors defined in the theoretical framework of the Quantum Theory of Atoms in Molecules (QTAIM)⁴¹ and the Non-Covalent Interactions (NCI) index⁴² to successfully analyze NCIs in gold compounds.^{32,43} Indeed, the QTAIM and NCI-index methodologies have also given valuable insights in the study of different non-covalent interactions, as π -stacking and hydrogen-bonds, which are also relevant for the systems addressed herein.⁴⁴⁻⁴⁶

Here we characterize thoroughly the prevalent interactions in the crystalline supramolecular architectures of a dozen compounds with the formula [Au(SR_F)(Ph₃P)] where Ph₃P = triphenylphosphine and SR_F = SC₆F₅ (**1**), SC₆HF₄₋₄ (**2**), SC₆F₄(CF₃)-4 (**3**), SC₆H₃F_{2-2,4} (**4**), SC₆H₃F_{2-3,4} (**5**), SC₆H₃F_{2-3,5} (**6**), SC₆H₄(CF₃)-2 (**7**), SC₆H₄F-2 (**8**), SC₆H₄F-3 (**9**), SC₆H₄F-4 (**10**), SCF₃ (**11**) and SCH₂CF₃ (**12**) (Scheme 1). We point out that the X-Ray structures of compounds **3** – **12** have not been reported before. The analysis of these structures reveals that changes in the fluorination of the thiolate group coordinated to the gold atom affect very strongly the prevalence of aurophilic interactions as a result of two effects. First, by means of the electronic modulation that the electronegative fluorine atoms exert over the metal centers and second, via the promotion of different supramolecular arrangements wherein the fluorinated moieties act as synthons, in this case, π -stacking and hydrogen-bonding. The QTAIM and NCI-index electron density analyses allow us to quantify and visualize the gradual variation in strength of the different interactions directing the crystal packing in the investigated compounds. Overall, this research reveals how the

structural modulation of aurophilic and other significant supramolecular interactions can be achieved by means of fluorination.



Scheme 1. Compounds addressed in this work.

RESULTS AND DISCUSSION

Compounds **1-12** were synthesized by substitution of chlorine with the corresponding thiolate group from the previously reported compound [AuCl(Ph₃P)] (synthetical details are given in the Experimental Section). Single crystal X-ray diffraction structures of all twelve compounds were determined by analyzing samples obtained by slow evaporation from acetone solutions. Although the structures of compounds **1** and **2** were previously reported,^{47,48} we have obtained and analyzed our own X-ray diffraction data. We proceeded in this way to maintain the same experimental conditions of crystallization and analysis in all the compounds addressed in this investigation. Our determined structures of **1** and **2** agree with previous reports.

In general, all compounds present the expected molecular geometry, in which the gold atom exhibits a linear coordination environment, with P-Au-S angles in the interval of 169° to 180°. The

largest deviations from linearity are observed in the compounds with Au...Au contacts. Bond distances are also in the typical ranges. Molecular ORTEP diagrams and structural information are available in the SI. Despite these similarities in molecular structure, the crystalline arrangements of the examined compounds present notorious diversity in the modes of interaction between molecular vicinal pairs. Our theoretical analyses of non-covalent interactions have allowed us to identify the most prominent contacts in the investigated compounds.

The main interactions which drive the crystalline arrangements in the twelve synthesized compounds are: π -stacking, hydrogen bonds and aurophilic contacts. They contend in the determination of the crystal packing of the systems under examination. We analyze the crystalline structures by identifying the main non-covalent interactions in dimers of the molecules considered herein. This identification is made via X-ray diffraction structures and NCI-index maps. Our analyses also provide insights about the factors promoting the observed interactions and include a quantitative assessment of the strength of the different interactions using several descriptors defined within the theoretical framework of the QTAIM, e.g. the delocalization index (DI). We proceed now to discuss the architectures assembled mainly by π -stackings then by H-bonds to finally consider those bonded by aurophilic contacts.

Architectures directed by π -stacking.

One of the most significant manifestation of π -stacking in our compounds is the π - π_F interaction which involves aryl-fluoroaryl contacts whose associated formation energies are reported to be about 20-25 kJ·mol⁻¹. Nevertheless, weaker (10-15 kJ·mol⁻¹) π - π and π_F - π_F interactions can also be found.⁴⁹⁻⁵² In turn, π - π_F interactions can possibly impair aurophilic contacts. The highly fluorinated phenylthiolate derivatives **1** and **2** show crystalline dispositions determined by the formation of π -stacking interactions and hence aurophilic contacts are totally suppressed. The left

side of Figure 1 shows the formation of dimeric units linked by two symmetry equivalent π - π_F interactions. The fluorophenyl ring on the thiolate fragment interacts with one of the vicinal phosphine phenyl groups. This arrangement was previously analyzed in terms of the quadrupolar model of π -stacking interactions.^{47,48} Additionally, these dimeric units are held together via other stacking interactions of the type π_F - π_F and π - π as observed in the right side of Figure 1. Table 1 reports some selected distances used to characterize these interactions within the crystal.

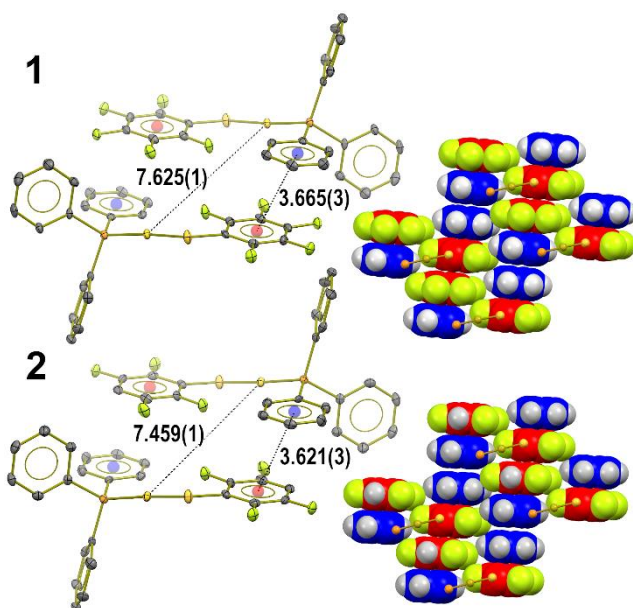


Figure 1. Left: formation of π_F - π stacked dimers of compounds **1** (top) and **2** (bottom). Hydrogen atoms are omitted for clarity. Right: view along the *c* crystallographic axis showing the packing of four of those dimeric π_F - π bonded assemblies held together also by π - π and π_F - π_F stackings. Fluorinated and non-fluorinated rings are displayed in red and blue colors respectively. Distances are indicated in Å.

Table 1. Distances used to characterize the π -stacking interactions in compounds **1** and **2**.

distances /Å	Compound 1			Compound 2		
	$\pi_F-\pi$	$\pi_F-\pi_F$	$\pi-\pi$	$\pi_F-\pi$	$\pi_F-\pi_F$	$\pi-\pi$
$d_{\text{centroids}}$	3.665(3)	3.624(3)	4.260(3)	3.621(3)	3.581(3)	4.356(3)
d_{split}	1.612(2)	1.152(1)	2.281(2)	1.357(1)	1.232(2)	2.289(1)
$d_{\text{interplanar}}$	3.291(2)	3.436(2)	3.598(2)	3.365(2)	3.373(2)	3.706(1)

Hereof, compound **3** which holds the relatively steric $-\text{CF}_3$ group would not, in principle, present an effective π -stacking as those observed in systems **1** and **2**. Nevertheless, the crystalline network of **3** has a similar pattern to **1** and **2**. Indeed, $\pi-\pi_F$ contacts occur in the dimeric units of **3** although displacements and angles between the stacked rings reveal a weaker interaction than those displayed in **1** and **2** (Figure 2). While compounds **1** and **2** show larger $\text{Au}\cdots\text{Au}$ distances (7.6253(7) and 7.4596(7) Å), the impairment of the $\pi-\pi_F$ stacking interactions in compound **3** leads to a very substantial shortening in the gold-gold distance ($d_{\text{Au}\cdots\text{Au}} = 3.5068(6)$ Å) which stands in the frontier of aurophilic distances (≤ 3.5 Å).¹⁸ The secondary $\pi-\pi$ and $\pi_F-\pi_F$ interactions displayed in the dimers of **1** and **2** almost disappear in system **3** whose dimers are instead held together by several $\text{F}\cdots\text{H}$ contacts between fluorinated and unfluorinated rings. The weakening of the π -stacking interactions in compound **3** due to steric hindrance allows for other non-covalent interactions within the system such as $\text{C-H}\cdots\text{F}$ and aurophilic contacts to stand out.

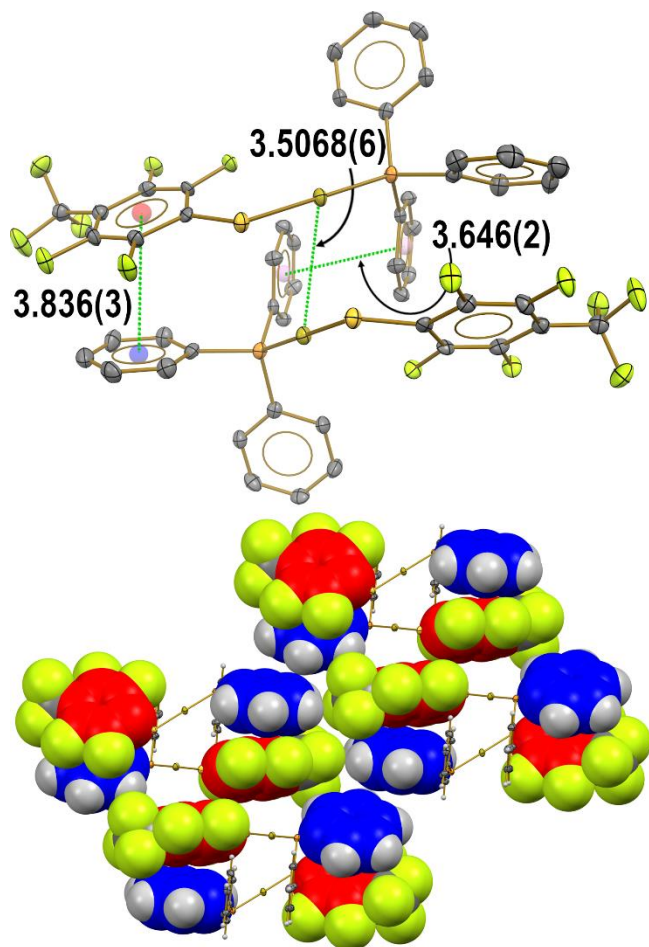


Figure 2. Top. Dimeric unit observed in the crystalline arrangement of compound **3**. The figure displays two main types of interaction, π - π_F and aurophilic contacts. Hydrogen atoms are omitted for clarity. Distances are indicated in Å. Bottom. General view along the *b* crystallographic axis showing the packing of four of those dimeric units mainly directed by H \cdots F contacts. Fluorinated and unfluorinated rings are displayed in red and blue respectively.

We consider now the wavefunction analyses of the dimers of **1-3**. The NCI-index maps reveal the locations where weak interactions take place within these systems (Figure 3). On one hand, the most important interaction surfaces in the dimers of compounds **1** and **2** are located in regions between fluorinated and unfluorinated phenyl groups. On the other, the analysis of compound **3** dimer shows notably more disperse surfaces for the π - π_F regions, an indication of weaker

interactions. The NCI-index analysis reveals several additional interactions in **3**. First, there is an extra π -stacking which involves the phosphine phenyl rings (Figure 3 inset (i)). Second, there is a clear NCI surface between the Au atoms which confirms a weak aurophilic contact (Figure 3 bottom-left). In short, the strength of the Au \cdots Au interactions investigated herein is modulated by their competition with π - π_F contacts. Third, we identify an intramolecular Au \cdots F contact that can be equally observed in **1** and **2** (Figure 3, inset (ii)). The Au \cdots F distances as well as the descriptors of these interactions based on the topology of the electron density are in agreement with our previous reports concerning the dominant closed-shell nature of these contacts (Figure S3 and Table S1).^{32,43}

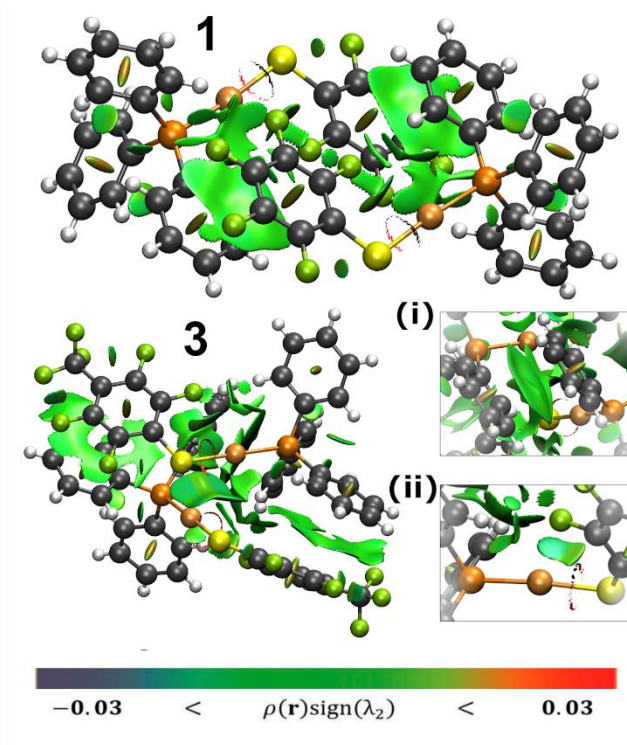


Figure 3. NCI-index isosurfaces which characterize the interactions within the dimers of **1** (top) and **3** (bottom-left). The insets in the bottom-right show a detail of (i) the secondary $\pi\cdots\pi$ interactions in **3** and (ii) the Au \cdots F intramolecular contact in **2**. The isosurface value of the reduced

density gradient is $s = 0.5$ a.u. and the values of ρ satisfy the condition $\rho \leq 0.015$ a.u. The scale for the relative magnitude of the interactions is presented at the bottom of the figure.

Concerning compounds **4-10**, π -stacking interactions are not the principal factors in the crystalline packing in these systems. Figure 4 shows the NCI-index analyses of dimeric aggregates of compounds **6**, **7** and **9** which display π - π_F stacking interactions that are clearly weaker than those found in systems **1-3**. Nevertheless, the reduction of the fluorination degree of the π_F rings in systems **6**, **7** and **9** increases the strength of H-bond interactions. On the other hand, the increase of the electron density in the gold atoms within compounds **4**, **5**, **8** and **10** results in architectures directed by aurophilicity (*vide infra*).

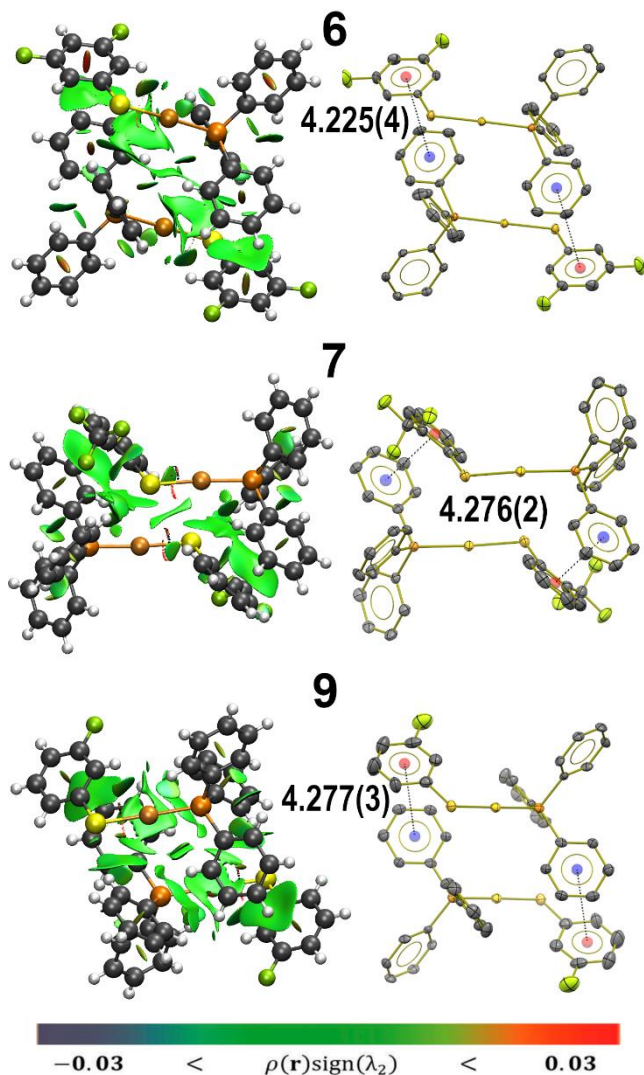


Figure 4. NCI-index isosurfaces (left) and ORTEP diagrams (right) which characterize the $\pi \cdots \pi_F$ -stacking interactions within the dimers of **6** (top), **7** (medium) and **9** (bottom). The isosurface value of s equals 0.5 a.u. and the electron density is such that $\rho \leq 0.015$ a.u. The scale for the relative magnitude of the interactions is presented at the bottom of the figure. Distances are indicated in Å.

The analysis of the electron delocalization index (DI) as defined by the QTAIM allows us to evaluate the covalent contributions of the corresponding interactions. The delocalization index quantifies the number of electron pairs (and hence covalency) shared between two atoms or groups

of atoms in real space. The DI values for the most important interactions observed in the dimers presenting π -stacking are reported in Table 2. The π - π_F interactions in **1** and **2** are associated with high values of DI while those measured for compound **3** are considerably smaller in agreement with the NCI-index analyses. The determined DIs reveal also that the weakening of the π - π_F stacking in compound **3** results in other non-covalent interactions. For example, the DIs associated with the π - π stacking which involves the lateral phosphines of **3** (0.19 a.u.) are comparable with those of the π - π_F moieties in **1** and **2** (Table 2). Most importantly, the DI between the gold centers in **3** (0.12 a.u.) indicates a weak aurophilic contact. Furthermore, if we consider the whole $(\text{Au}\cdots\text{S})_2$ fragment, the total intermolecular DI is significantly larger (0.46 a.u.). This result indicates a significant contribution of the $\text{Au}\cdots\text{S}$ interactions to the intermolecular bonding of the **3** dimer.

Table 2. Delocalization indices and geometrical parameters used to characterize π_F - π -stacking interactions in the dimers of **1-10**.

Compound	$\text{DI}_{\pi_F-\pi}^1$ / a.u.	$d_{\text{centroids}}$ / Å	$\Theta_{\pi_F-\pi}^{\text{o}2}$	Main interaction
1	0.298	3.665(3)	1.6	π_F - π
2	0.285	3.621(3)	2.3	π_F - π
3	0.246	3.836(3)	21.1	π_F - π /aurophilic
4	0.121	4.214(4)	25.1	aurophilic
5	0.178	3.983(3)	8.97	aurophilic
6	0.129	4.225(4)	27.5	H-bond
7	0.139	4.277(3)	34.9	H-bond
8	0.124	4.209(2)	23.9	aurophilic
9	0.130	4.276(2)	29.9	H-bond
10	0.103	4.812(3)	42.1	aurophilic

¹This value takes into account all the C, H and F atoms in the interacting phenyl groups. ²Dihedral angle between the π_F and π planes.

The DI values for the π_F - π -stacking interactions in the dimers of compounds **4-10** are considerably lower than those in systems **1-3**, in agreement with the weaker interaction in the former set of molecules due to the smaller fluorination degree of their π_F rings. The fluorination pattern in compounds **6**, **7** and **9** is suitable for the occurrence of H-bonded structures. The transfer of electron density to the gold centres in compounds **4**, **5**, **8** and **10** strengthen the Au \cdots Au contacts even to the point that aurophilic interactions overcome π - π_F stacking. Our results point out that **3** is a borderline case in which the π - π_F interactions having DI values of around 0.24 a.u. compete with aurophilic contacts. The nature of the Au \cdots Au contact in **3** will be further described below.

Hydrogen-Bonded Architectures.

Compounds **6**, **7**, **9**, **11** and **12** present C-H \cdots F, C-H \cdots S or C-H $\cdots\pi$ ⁵³ H-bonds. Systems **6** and **9** present the fluorination of the thiolate ring only in the *meta* positions. The motif formed in the dimeric structures of compounds **6** and **9** is similar to that found by Desiraju⁵⁴ in fluorinated benzenes. The acidity of the *ortho* hydrogen of the phenyl of the thiolate ligand in these molecules is increased by the α -influence of fluorine and sulfur. Therefore, cyclic structures occur that give rise to dimeric units with H \cdots F contacts as revealed by NCI-index analyses (Figure 5). Other non-covalent contacts that are relevant for the formation of the dimers of **6** and **9** are H $\cdots\pi$ interactions between one phenyl ring on the phosphine and the *para* hydrogen of the fluorothiolate. These interactions are revealed as cone-shaped surfaces in the NCI-index analysis shown in Figure 5.

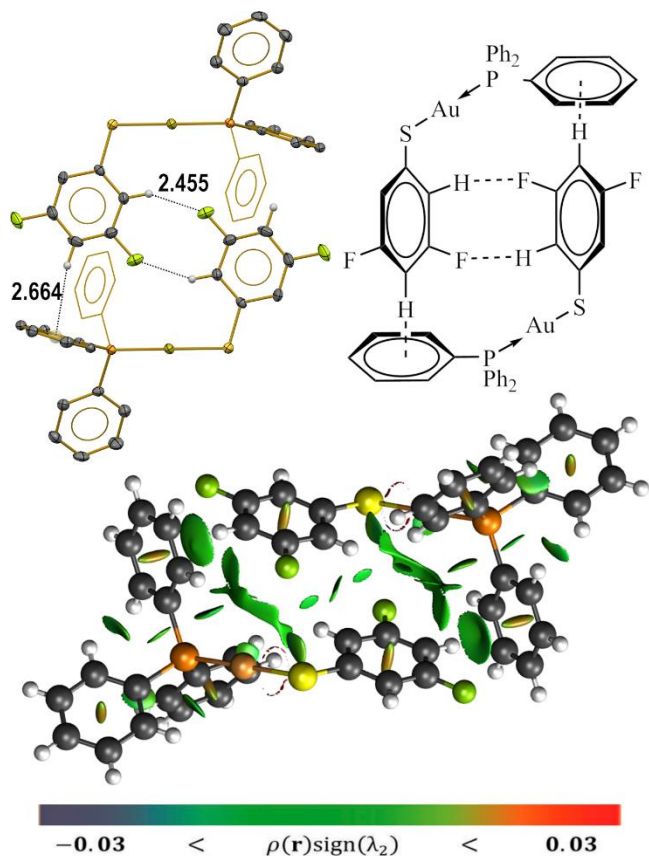


Figure 5. C-H \cdots F/C-H \cdots π bridged motifs observed in the dimer of **6**. We show the crystal structure of this compound (top-left), a schematic representation of the interactions within the corresponding dimer (top-right) and the NCI-index isosurfaces within a dimer of **6** (bottom). The s isosurface value equals 0.5 a.u. The values of the electron density are such that $\rho \leq 0.015$ a.u. The scale for the relative magnitude of the interactions is presented at the bottom of the figure. Similar results are found for the dimer of **9**. Distances are indicated in Å.

Table 3 shows selected quantum chemical topology parameters for the A \cdots H (A = F, S, π) interactions in the dimers of compounds **6** and **9**. Besides DIs, the electron density at the Bond Critical Point ($\rho(\mathbf{r}_{\text{BCP}})$) has also been used to quantitatively assess the strength of chemical interactions. The H \cdots F contacts observed in the dimer of the difluorinated compound **6** show a DI of 0.027 a.u., with a value of $\rho(\mathbf{r}_{\text{BCP}}) = 0.007$ a.u., while in the dimer of the monofluorinated

compound **9** the corresponding values of DI are 0.019 a.u. with $\rho(\mathbf{r}_{\text{BCP}}) = 0.005$ a.u. Thus, the crystalline arrangement is most compact and presents stronger H \cdots F contacts in system **6**. This observation can be rationalized in terms of the enhanced acidity of the protons because of the inductive effects of the double fluorination in **6**. Table 3 also presents the quantum chemical topology parameters for other kind of H \cdots A contacts obtained for the dimers of compounds **7**, **11** and **12**. System **7** shows several weak C-H \cdots F interactions (Figure S4). Given the expected greater proton affinity of aliphatic over aromatic fluorine atoms,^{54,55} **11** and **12** display even stronger H \cdots F contacts (Figures 6 and S5).⁵⁶ The NCI-index analysis in compound **12** reveals another H \cdots π contact as typical cone-shaped surfaces among different rings of the PPh₃ fragments (Figure 6). The distance of the H atom to the phenyl plane in that interaction is 2.642 Å and the calculated DI for the contact is 0.65 a.u. which indicates a particularly strong interaction, comparable to that among water monomers in H₂O clusters.⁵⁷ The Laplacian of the electron density at the bond critical points ($\nabla^2\rho(\mathbf{r}_{\text{BCP}})$) corresponding to all the above-mentioned A \cdots H interactions are small and positive, a condition which indicates the closed shell character of these contacts.

Table 3. QTAIM indicators and distances for selected H \cdots A (A = F, S, π) interactions in dimers of the systems **6**, **7**, **9**, **11** and **12**.

Compound	Contact	DI _{H\cdotsA} / a.u.	$\rho(\mathbf{r}_{\text{BCP}})$ / a.u.	$\nabla^2\rho(\mathbf{r}_{\text{BCP}})$ / a.u.	$d_{\text{H}\cdots\text{A}}$ / Å
6	H \cdots F	0.027	0.007	0.0312	2.455
	H \cdots π	0.063	-	-	2.664
	H \cdots S*	0.032	0.007	0.0206	3.145
7	H \cdots F	0.015	0.004	0.0130	2.732
	H \cdots S	0.023	0.006	0.0169	3.068

9	H···F	0.019	0.005	0.0202	2.631
	H··· π	0.056	-	-	2.752
	H···S*	0.025	0.006	0.0204	3.155
11	H···F	0.026	0.007	0.0318	2.507
	H···S	0.032	0.006	0.0179	3.024
12	H···F	0.020	0.005	0.0185	2.654
	H··· π	0.065	-	-	2.642

When the system presents more than one of the indicated type of interaction, we report only the value which corresponds to the contact with the largest DI.

* The indicated contact is an S··· σ_{C-H} interaction rather than an H-bond.

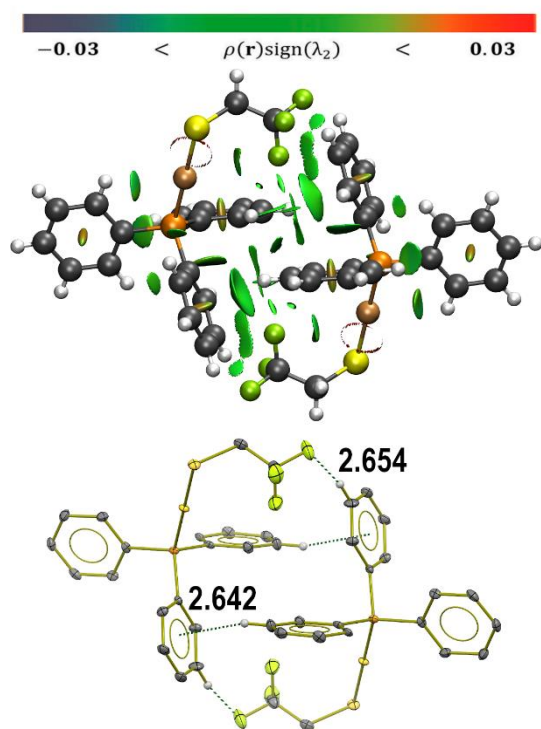


Figure 6. Top: Principal interactions revealed by the NCI-index analysis in compound **12**. The isosurface value of s equals 0.5 a.u. and the electron density is such that $\rho \leq 0.015$ a.u. The scale

for the relative magnitude of the interactions is presented in the top of the figure. Bottom: Selected H···A distances in the system. The distances are reported in angstroms.

The dimers of systems **6**, **7**, **9** and **11** present H···S contacts. These interactions in **6** and **9** are not hydrogen bonds but agostic-like S··· $\sigma_{\text{C-H}}$ interactions as the bond paths associated with these contacts finish at the C-H bond critical points⁵⁸ (Figure 7). Although the DIs between H and S are small, the total DIs between the S atom and the C-H fragments are not negligible (0.057 and 0.044 a.u. for **6** and **9** respectively). Similarly to the H···F contacts, these H···S interactions are slightly stronger and shorter in **6** than they are in **9** (Table 3). The values of $\nabla^2\rho(\mathbf{r}_{\text{BCP}})$ indicate that the interactions are predominantly closed shell in nature. There are bond paths in the dimers of compounds **7** and **11** associated with H···S contacts which are also closed shell interactions.

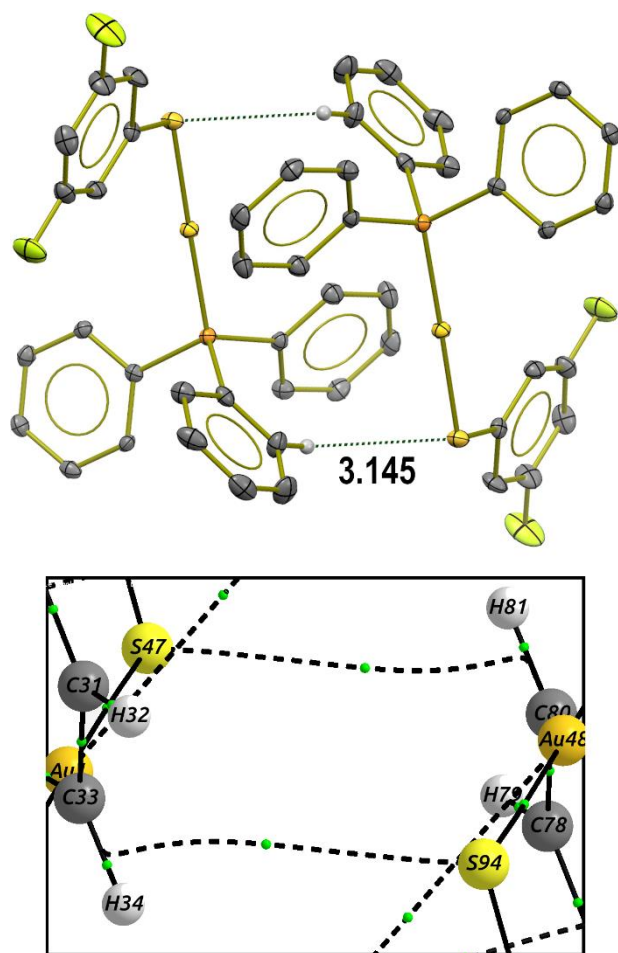


Figure 7. S \cdots H interactions in the dimer of **6** (top) along with the corresponding bond paths (bottom). The indicated H \cdots S distance is reported in Å.

Overall, H-bonds and π -stacking contacts prevent the formation of aurophilic interactions which otherwise are formed with other fluorination patterns as discussed in the following section.

Architectures with aurophilic interactions

Aurophilic contacts turn out to be the prevalent driving force in the stabilization of the crystalline arrangement of the moderately fluorinated compounds **4**, **5**, **8** and **10**. The blue surfaces in the NCI-index analyses of the dimers of these compounds indicate strong Au \cdots Au interactions (Figure

8). These analyses also reveal π - π_F contacts that, as previously mentioned, are not strong enough to impair the formation of aurophilic contacts in these systems. As opposed to the nearly parallel arrangement of the previously discussed dimers of predominant π -stacked and H-bonded architectures, the conformations of systems **4**, **5**, **8** and **10** in their dimers match those expected for aurophilic arrangements.⁴⁰ Namely, we observe S/Au/Au/S torsion angles equal to 87.1°, 93.5°, 90.3° and 94.9° for **4**, **5**, **8** and **10** respectively. Table 4 reports some topological properties of the electron density used to characterize these aurophilic contacts. The QTAIM analyses reveal that the examined Au \cdots Au interactions are moderately covalent: the values of $\rho(\mathbf{r}_{\text{BCP}})$ and $\nabla^2\rho(\mathbf{r}_{\text{BCP}})$ are generally small, the total energy densities $H(\mathbf{r}_{\text{BCP}})$ are slightly negative and the ratios $|V(\mathbf{r}_{\text{BCP}})|/G(\mathbf{r}_{\text{BCP}})$ are greater than one.⁵⁹ The incipient Au \cdots Au contact in the dimer of **3** is weaker than those in the rest of the investigated compounds and it has a different character, as revealed by the corresponding smaller values of DI, $\rho(\mathbf{r}_{\text{BCP}})$ and $\nabla^2\rho(\mathbf{r}_{\text{BCP}})$ and the fact that the quotient $|V(\mathbf{r}_{\text{BCP}})|/G(\mathbf{r}_{\text{BCP}})$ is less than one. Accordingly, the small, yet negative, charges of the gold atoms of **3** explain the incipient formation of the Au \cdots Au contact in this dimer. This interaction does not prevail over the rest of intermolecular contacts in this system and, thus, its role is secondary in the mainly π -stacked architecture discussed previously.

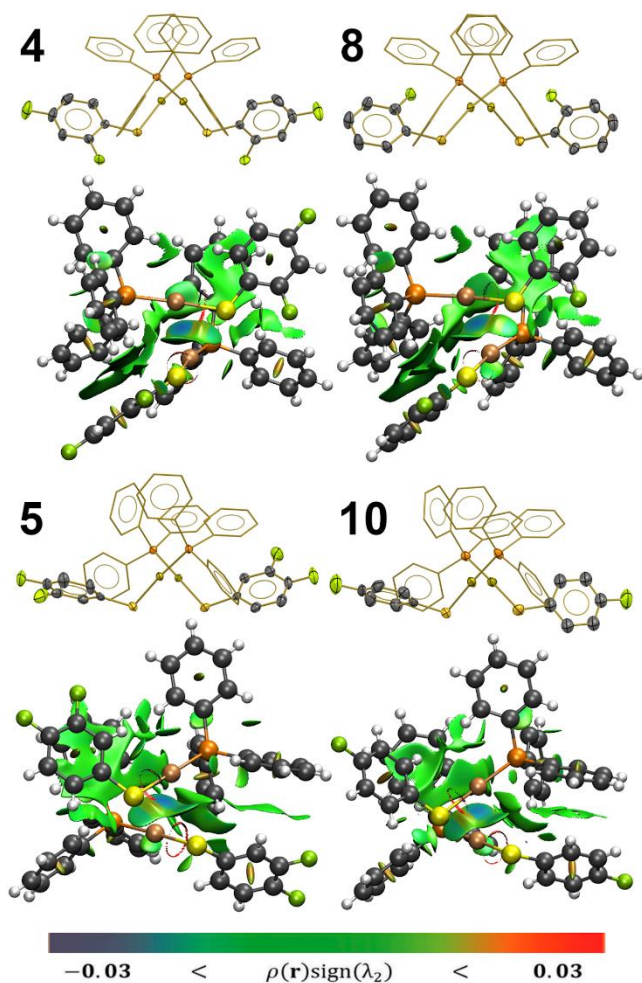


Figure 8. X-ray diffraction structures and NCI-index analyses of the dimers of compounds **4**, **5**, **8** and **10**. The NCI plots indicate aurophilic contacts and secondary π -stacking interactions. The Au \cdots Au distances are 3.0787(5), 3.1010(4), 3.1019(5) and 3.1140(5) Å for systems **4**, **5**, **8** and **10** respectively. The isosurface value of the reduced density gradient is $s = 0.5$ a.u. and the values of ρ satisfy the condition $\rho \leq 0.015$ a.u. The scale for the relative magnitude of the interactions is presented at the bottom of the figure.

Table 4. QTAIM descriptors and experimental distances for the Au \cdots Au interactions observed in this work.

System	$q_{\text{Au1/a.u.}}$	$q_{\text{Au2/a.u.}}$	$\text{DI}_{\text{Au}\cdots\text{Au}}$	$\rho(\mathbf{r}_{\text{BCP}})$	$\nabla^2\rho(\mathbf{r}_{\text{BCP}})$	$H(\mathbf{r}_{\text{BCP}})$	$ V(\mathbf{r}_{\text{BCP}}) /$ $G(\mathbf{r}_{\text{BCP}})$	$G(\mathbf{r}_{\text{BCP}})$ $/\rho(\mathbf{r}_{\text{BCP}})$	$d_{\text{Au}\cdots\text{Au}}/\text{\AA}$
3	-0.01	-0.01	0.119	1.34E-02	3.13E-02	+0.0005	0.93	0.54	3.5068(6)
4	-0.05	-0.04	0.280	2.80E-02	7.12E-02	-0.0011	1.06	0.68	3.0787(5)
5	-0.05	-0.05	0.260	2.69E-02	6.86E-02	-0.0009	1.05	0.67	3.1010(4)
8	-0.04	-0.04	0.277	2.69E-02	6.84E-02	-0.0008	1.05	0.67	3.1019(5)
10	-0.05	-0.05	0.257	2.62E-02	6.70E-02	-0.0007	1.04	0.67	3.1140(5)
SPh*	-0.04	-0.04	0.246	2.43E-02	6.15E-02	-0.0004	1.03	0.65	3.155 (2)

*[Au(SPh)(PPh₃)]⁶⁵

As recently stated by Dem'yanov,³⁸ electron-rich gold centers tend to form relatively strong Au \cdots Au contacts but the relation between charge-density and the energetics of aurophilic interactions is not straightforward. The system with the largest DI(Au \cdots Au), and correspondingly the stronger interaction, is the dimer of the difluorinated compound **4**. We note that the strength of the interaction decreases with the change in the fluorination pattern in **5** and with the removal of a fluorine atom in **8** and **10**. Furthermore, the dimer of the unfluorinated derivative [Au(SPh)(PPh₃)] has a larger Au \cdots Au distance (3.155(2) Å)⁶⁰ and smaller values of DI, $\rho(\mathbf{r}_{\text{BCP}})$ and $\nabla^2\rho(\mathbf{r}_{\text{BCP}})$. These conditions indicate a weaker aurophilic interaction in the dimer of the last-mentioned compound. Therefore, the strengthening of aurophilic contacts might result not only from an increase of the electron population over the gold centers but also from a slight degree of fluorination in the system. This observation can be understood by considering Au \cdots Au contacts as donor-acceptor interacting pairs.^{33,34} In this way, the electronic population of gold atoms characterizes the capabilities of these centers as donors while the light fluorination of the thiolate improves their efficiency as acceptors.

In summary, we analyzed how the fluorination in thiolate ligands can modify the crystalline self-association of gold(I) compounds. The relative strength of the different interactions in each system

has been quantified by means of several QTAIM descriptors, in particular by DIs. While phenyl groups are present in all compounds and thus π -stacking interactions may occur, simple phenyl π - π stacking motifs (DI < 0.2 a.u.) are secondary with respect to H \cdots F and Au \cdots Au contacts. The introduction of stronger π -stacking synthons as the highly fluorinated rings allows the formation of stronger π - π_F interactions (DI > 0.2 a.u.) which overcome the H \cdots F and Au \cdots Au contacts. These observations provide a valuable tool for the tuning of aurophilic contacts and illustrates how the experimental and theoretical approach followed in this research proves useful in the quantitative assessment of the strength of non-covalent interactions in compounds containing gold atoms. Furthermore, the examined systems are of broad interest for inorganic chemists as PPh₃ is a model for the wide range of phosphines used as ligands for gold complexes. Additionally, the thiolate pseudohalogen nature not only provides stability to the studied compounds but it also allows for an electronic modulation of the interactions discussed in the paper via the fluorinated moiety.

CONCLUSIONS

The analysis of a series of gold(I) compounds bearing triphenylphosphine and fluorinated thiolates illustrates how to rationally modulate the formation of aurophilic contacts via their supramolecular competition with π - π_F stacking and H-bond interactions. While highly fluorinated systems favor the formation of strong π -stacking interactions unless strongly steric groups interfere as they do in compound **3**, a decrease in the fluorination degree allows the formation of aurophilic contacts except if the fluorination pattern promotes the formation of C-H \cdots F motifs. QTAIM analyses indicate that π -stacked architectures prevail when large electron delocalization occurs for the involved rings (between 0.24 and 0.30 a.u.). When this electron delocalization decreases, H \cdots F and aurophilic contacts arise. The latter become dominant when the DI between the gold atoms is larger than 0.2 a.u. In general, the preference on interactions follows the order π - π_F > H \cdots F >

$\text{Au}\cdots\text{Au} > \pi\text{-}\pi$. The fluorination of the ligands exerts electronic effects that contribute to the modulation of aurophilic contacts and other non-covalent interactions. Besides the previous evidence which supports that electron rich gold centers form strong $\text{Au}\cdots\text{Au}$ contacts, our results indicate that the acceptor character of the gold centers might also strengthen these interactions. This donor-acceptor interplay between the gold centers can also be moderated by the degree of fluorination of the ligands. Overall, the results of this investigation yield valuable insights in the design of supramolecular building blocks of Au(I) complexes.

EXPERIMENTAL SECTION

All the chemicals and deuterated solvents were purchased from commercial sources and used without further purification. Regular solvents were dried using standard Schlenk techniques. Caution! Lead is a highly toxic heavy metal; it must be used carefully, and residual derivatives should be properly disposed. Thiols and thiolates are highly smelly and must be manipulated in fume hoods.

Instrumentation. Infrared spectra were measured on a Perkin-Elmer FTIR/FIR Spectrum 400 spectrometer in the range of 4000 to 400 cm^{-1} via Attenuated Total Reflectance (ATR). Elemental analyses were determined utilizing a Thermo Scientific Flash 2000 Analyser at 950°C. ^1H and ^{13}C NMR spectra were recorded on a 9.4 T Varian VNMRS spectrometer while ^{19}F and ^{31}P NMR were obtained on a 7.0 T Oxford Spectrometer. Chemical shifts are in ppm relative to TMS with $\delta = 0$ ppm internal reference for ^1H , ^{13}C and to external references of H_3PO_4 for ^{31}P and CFCl_3 for ^{19}F at 0 ppm. The coupling constants values are given in Hz. Positive-ion fast atom bombardment spectra (MS-FAB⁺) were measured on an MStation JMS-700 mass spectrometer operated at an

acceleration voltage of 10 kV. Samples were desorbed from a 3-nitrobenzyl alcohol matrix by 3 keV xenon atoms employing the matrix ions as the reference material.

Synthesis. Lead thiolates $\text{Pb}(\text{SR}_F)_2$ used in the synthesis of the compounds examined herein, were obtained by the reaction of stoichiometrical amounts of aqueous lead acetate ($\text{Pb}(\text{CH}_3\text{COO})_2$) with a concentrated solution of the corresponding thiol in methanol, yielding a yellow or white ($\text{SR}_F = \text{SC}_6\text{HF}_4, \text{SCH}_2\text{CF}_3$) solid that was thoroughly washed with water and hexane.⁶¹ Silver(I) trifluoromethylthiolate, obtained as described in Reference 62, was used in the synthesis of **12** because of the instability of the lead analogue. The compound $[\text{AuCl}(\text{PPh}_3)]$ was obtained by the direct reaction of $\text{K}[\text{AuCl}_4]$ with PPh_3 as reported by Fackler⁶³. The synthesis and characterization of compounds **1**, **3**, **11** and **12** were previously reported.^{64,65} The syntheses of all the new compounds were carried in a similar manner, thus only the synthesis of **2** is described in detail.

Compound 2 $[\text{Au}(\text{SC}_6\text{HF}_4)(\text{PPh}_3)]$. 200 mg (0.404 mmol) of $[\text{AuCl}(\text{PPh}_3)]$ were dissolved in 20 mL of CH_2Cl_2 in a 50 mL round bottom flask. Later, a stoichiometrical amount (0.202 mmol) of solid lead thiolate was added and the mixture was stirred at room temperature for 12 hours. Afterwards, a white precipitate powder (PbCl_2) was formed and the reaction mixture was filtered, and the liquid fraction volume reduced to 5 mL by low pressure evaporation. The product precipitates as a pale yellowish crystalline powder after the addition of 20 mL of hexane to the system. Yield 89.1 % (0.2307 g, 0.360 mmol); m. p. 165 - 167°C. Anal. Calcd. for $\text{C}_{24}\text{H}_{16}\text{AuF}_4\text{PS}$: C, 45.01; H, 2.52; S, 5.01. Found: C, 45.11; H, 2.57; S, 4.98. IR (cm^{-1}): 1478.83, 1428.41, 1163.40, 1100.16, 910.79, 884.15, 689.98. MS (FAB⁺; m/Z) $[\text{M}]^+$ 640 (13 %), $[\text{M}-\text{SC}_6\text{F}_4\text{H}]^+$ 459 (100 %), $[\text{M}+\text{Au}(\text{PPh}_3)]^+$ 1099 (100 %). ¹H-NMR (CDCl_3 , 400 MHz) δ 7.58-7.43 (m, 15H, PPh_3), 6.69 (m, 1H, H- $\text{C}_6\text{F}_4\text{H}$). ¹⁹F-NMR (CDCl_3 , 282.4 MHz) δ -132.94 (m, 2F, o-F- $\text{C}_6\text{F}_4\text{H}$), -141.27 (m, 2F, m-F- $\text{C}_6\text{F}_4\text{H}$). ³¹P-NMR (CDCl_3 , 121.5 MHz) δ 37.7 (s, 1P, PPh_3).

Compound 4 [Au(SC₆H₃F₂-2,4)(PPh₃)]. Yield 90.0 % (0.2174 g, 0.360 mmol). m. p. 140 - 142°C. Anal. Calcd. for C₂₄H₁₈AuF₂PS: C, 47.69; H, 3.00; S, 5.30. Found: C, 47.66; H, 3.05; S, 5.26. IR (cm⁻¹): 3072.17, 3058.66, 1477.49, 1434.46, 1132.73, 1100.85, 746.86, 689.27. MS (FAB⁺; *m/z*) [M]⁺ 604 (22 %), [M-SC₆F₂H₃]⁺ 459 (84 %), [M+Au(PPh₃)]⁺ 1063 (100 %). ¹H-NMR (CDCl₃, 400 MHz) δ 7.58 (m, 1H), 7.57 - 7.42 (m, 15H, PPh₃), 6.75 (m, 1H), 6.67 (m, 1H). ¹⁹F-NMR (CDCl₃, 282.4 MHz) δ -100.37 (m, 1F, o-F-C₆H₃F₂), -116.86 (m, 1F, p-F-C₆H₃F₂). ³¹P-NMR (CDCl₃, 121.5 MHz) δ 38.2 (s, 1P, PPh₃).

Compound 5 [Au(SC₆H₃F₂-3,4)(PPh₃)]. Yield 89.7 % (0.2192 g, 0.363 mmol). m. p. 140 - 142°C. Anal. Calcd. for C₂₄H₁₈AuF₂PS: C, 47.69; H, 3.00; S, 5.30. Found: C, 47.71; H, 3.10; S, 5.25. IR (cm⁻¹): 3070.24, 3046.34, 1590.55, 1490.02, 1480.20, 1434.67, 1267.45, 1099.30, 744.72, 690.38. MS (FAB⁺; *m/z*): [M]⁺ 604 (20 %), [M-SC₆F₂H₃]⁺ 459 (100 %), [M+Au(PPh₃)]⁺ 1063 (86 %). ¹H-NMR ((CD₃)₂SO, 400 MHz) δ 7.80 - 7.57 (m, 15H, PPh₃), 7.44 (m, 1H), 7.30 (m, 1H), 7.22 (m, 1H). ¹⁹F-NMR (CDCl₃, 282.4 MHz) δ -148.37 (m, 1F, m-F-C₆H₃F₂), -141.58 (m, 1F, p-F-C₆H₃F₂). ³¹P-NMR (CDCl₃, 121.5 MHz) δ 36.0 (s, 1P, PPh₃).

Compound 6 [Au(SC₆H₃F₂-3,5)(PPh₃)]. Yield 90.0 % (0.2171 g, 0.360 mmol). m. p. 161 - 162°C. Anal. Calcd. for C₂₄H₁₈AuF₂PS: C, 47.69; H, 3.00; S, 5.30. Found: C, 47.70; H, 3.08; S, 5.33. IR (cm⁻¹): 3072.52, 3059.52, 1602.32, 1575.69, 1479.25, 1433.57, 1101.19, 979.64, 746.83, 690.07. MS (FAB⁺; *m/z*): [M]⁺ 604 (25 %), [M-SC₆F₂H₃]⁺ 459 (100 %), [M+Au(PPh₃)]⁺ 1063 (100 %). ¹H-NMR (CDCl₃, 400 MHz) δ 7.77 - 7.60 (m, 15H, PPh₃), 7.15 (m, 2H, o-H-C₆H₃F₂), 6.86 (m, 1H, p-H-C₆H₃F₂). ¹⁹F-NMR (CDCl₃, 282.4 MHz) δ -114.88 (m, 2F, F-C₆H₃F₂). ³¹P-NMR (CDCl₃, 121.5 MHz) δ 33.1 (s, 1P, PPh₃).

Compound 7 [Au(SC₆H₄(CF₃)-2)(PPh₃)]. Yield 86.9 % (0.2238 g, 0.314 mmol). m. p. 149 - 151°C. Anal. Calcd. for C₂₅H₁₉AuF₃PS: C, 47.18; H, 3.01; S, 5.04. Found C, 47.22; H, 2.97; S,

4.99. IR (cm⁻¹): 1433.88, 1308.72, 1166.98, 1100.90, 1030.18, 997.30, 748.10, 691.90. MS (FAB⁺; *m/z*): [M]⁺ 637 (30 %), [M-SC₆H₄F]⁺ 459 (100 %), [M+Au(PPh₃)]⁺ 1095 (57 %). ¹H-NMR (CDCl₃, 400 MHz) δ 7.98 (m, 1H), 7.56 (m, 1H), 7.60 - 7.41 (m, 15H, PPh₃), 7.16 (m, 1H), 7.03 (m, 1H). ¹⁹F-NMR (CDCl₃, 282.4 MHz) δ -62.02 (s, 3F). ³¹P-NMR (CDCl₃, 121.5 MHz) δ 38.3 (s, 1P, PPh₃).

Compound 8 [Au(SC₆H₄F-2)(PPh₃)]. Yield 88.6 % (0.2100 g, 0.358 mmol). m. p. 144 - 145°C. Anal. Calcd. for C₂₄H₁₉AuFPS: C, 49.16; H, 3.27; S, 5.47. Found: C, 49.18; H, 3.33; S, 5.49. IR (cm⁻¹): 1467.99, 1461.46, 1434.46, 1208.36, 1099.69, 1067.84, 736.21, 688.35. MS (FAB⁺; *m/z*): [M]⁺ 586 (39 %), [M-SC₆H₄F]⁺ 459 (100 %), [M+Au(PPh₃)]⁺ 1045 (88 %). ¹H-NMR (CDCl₃, 400 MHz) δ 7.67 (m, 1H), 7.58 - 7.44 (m, 16H), 6.96 (m), 6.90 (m, 1H). ¹⁹F-NMR (CDCl₃, 282.4 MHz) δ -105.09 (s, 1F). ³¹P-NMR (CDCl₃, 121.5 MHz) δ 38.2 (s, 1P, PPh₃).

Compound 9 [Au(SC₆H₄F-3)(PPh₃)]. Yield 80.1 % (0.1900 g, 0.324 mmol). m. p. 151 - 153°C. Anal. Calcd. for C₂₄H₁₉AuFPS: C, 49.16; H, 3.27; S, 5.47. Found: C, 49.09; H, 3.31; S, 5.47. IR (cm⁻¹): 1594.38, 1567.01, 1463.10, 1433.05, 1098.57, 871.62, 742.62, 689.45. MS (FAB⁺; *m/z*): [M]⁺ 586 (39 %), [M-SC₆H₄F]⁺ 459 (100 %), [M+Au(PPh₃)]⁺ 1045 (95 %). ¹H-NMR (CDCl₃, 400 MHz) δ 7.60 - 7.41 (m, 16H), 7.33 (m, 1H), 7.03 (m, 1H), 6.67 (m, 1H). ¹⁹F-NMR (CDCl₃, 282.4 MHz) δ -114.57 (s, 1F). ³¹P-NMR (CDCl₃, 121.5 MHz) δ 38.5 (s, 1P, PPh₃).

Compound 10 [Au(SC₆H₄F-4)(PPh₃)]. Yield 89.2 % (0.2115 g, 0.361 mmol). m. p. 159 - 160°C. Anal. Calcd. for C₂₄H₁₉AuFPS: C, 49.16; H, 3.27; S, 5.47. Found: C, 49.20; H, 3.25; S, 5.54. IR (cm⁻¹): 1477.77, 1434.79, 1213.42, 1099.36, 1084.49, 823.18, 746.59, 691.64. MS (FAB⁺; *m/z*): [M]⁺ 586 (19 %), [M-SC₆H₄F]⁺ 459 (65 %), [M+Au(PPh₃)]⁺ 1045 (100 %). ¹H-NMR (CDCl₃, 400 MHz) δ 7.58 - 7.43 (m, 17H), 6.80 (m, 1H). ¹⁹F-NMR (CDCl₃, 282.4 MHz) δ -121.17 (s, F). ³¹P-NMR (CDCl₃, 121.5 MHz) δ 37.8 (s, 1P, PPh₃).

COMPUTATIONAL DETAILS

Electron densities and approximate pair densities of the systems examined herein were computed via Density Functional Theory using the X-Ray experimental structures with the aid of the Orca program.⁶⁶ More specifically, we used the BP86 exchange-correlation functional^{67,68} along with the TVZ-ZORA basis set⁶⁹ under the Zeroth Order Regular Approximation (ZORA).^{70,71} This method has proved to be accurate in its description of metal-metal and metal-ligand interactions in coordination and organometallic compounds. The resulting electron and pair densities were analyzed with the Quantum Theory of Atoms in Molecules (QTAIM), which provides a partition of the three-dimensional space in disjoint regions that are identified with atoms and functional groups in chemistry.^{41,72,73} The QTAIM is based on the electron distribution, a scalar field that equals the expectation value of a Dirac observable, i.e., $\rho(\mathbf{r}) = \langle \sum_{i=1}^N \delta(\mathbf{r}_i - \mathbf{r}) \rangle$ and therefore invariant under orbital rotations. This condition enables QTAIM to examine chemical bonding in different systems, e.g. π - π , H-bonded and donor-acceptor complexes⁷⁴ under the same physically-sound footing. The QTAIM analysis was performed with the AIMAll software.⁷⁵ Non-covalent interactions were further examined by considering the NCI index⁴² (a quantity based on the reduced gradient of the electron density), with the NCIPLOT program.⁷⁶ The visualization of chemical structures was made with the program VMD.⁷⁷

CRYSTAL STRUCTURE DETERMINATION

Suitable single crystals of compounds **1-12** were mounted on glass fibers and crystallographic data were collected at 130 K with an Oxford Diffraction Gemini "A" diffractometer with a CCD area detector with a monochromator of graphite for $\lambda_{\text{MoK}\alpha} = 0.71073 \text{ \AA}$. CrysAlisPro and CrysAlis RED software packages were used for data collection and integration.⁷⁸ The double pass method of scanning was used to exclude any noise. The collected frames were integrated by using an

orientation matrix determined from the narrow frame scans. Final cell constants were determined by global refinement. The absorbance in the collected data was considered via analytical and numeric corrections using a multifaceted crystal model based on expressions from the Laue symmetry with equivalent reflections.⁷⁹ Structure solutions and refinements were carried out with the SHELXS-2014 and SHELXL-2014 packages.^{80,81} The WinGX v2018.3⁸² software was used to prepare material for publication. Full-matrix least-squares refinements were carried out by minimizing $(Fo^2 - Fc^2)^2$. All non-hydrogen atoms were refined anisotropically. H atoms attached to C atoms were placed in geometrically idealized positions and refined as bonded on their parent atoms, with the C–H bond length equal to 0.95 and 0.99 Å for aromatic and methylene groups respectively and with $U_{iso}(H) = 1.2U_{eq}(C)$. In the structures of compounds **4** and **8** F1 and F1A are disordered over two sites with occupancies 0.63:0.37 and 0.51:0.49 respectively. Crystallographic data for all the investigated complexes is presented in Tables S1-S36 in the Supporting Information. The crystallographic data for the structures reported in this paper have been deposited in the Cambridge Crystallographic Data Centre with publication no. CCDC 1955689-1955700. Copies of the data can be obtained free of charge on application to CCDC, 12 Union Road, Cambridge, CB2 1EZ, UK (fax: (+44) 1223-336-033, e-mail: deposit@ccdc.cam.ac.uk)

ASSOCIATED CONTENT

The following files are available free of charge: Supplementary Information (PDF). Supporting Information Available: Supplementary figures and tables, Au-F interaction characterization, experimental NMR spectra and crystallographic tables.

AUTHOR INFORMATION

Corresponding Author

Guillermo Moreno-Alcántar, Institut de Science et d' Ingénierie Supramoléculaires (ISIS), University of Strasbourg. 8 Allée Gaspard Monge, 67083 Strasbourg Cedex, France. E-mail: morenoalcantar@unistra.fr

Present Addresses

Romero-Montalvo, Eduardo: Department of Chemistry, University of British Columbia, 3427 University Avenue, Kelowna, British Columbia V1V 1V7, Canada

Author Contributions

G.M.A. and H.T. designed the experimental work. G.M.A. and L.T.G. carried out the corresponding experiments. M.F.A. determined the crystal structures. J.M.G.V., E.R.M., A.M.P. and T.R.R. carried out the quantum chemical analyses. All authors contributed to the writing of the paper. All authors have given approval to the final version of the manuscript. J.M.G.V. and E.R.M. contributed equally to the work presented herein.

Funding Sources

We acknowledge financial support from DGAPA-UNAM IN210818, CONACYT-Mexico CB-2012/177498, as well as PhD scholarships 270993 and 472432 for J.M.G.V. and E.R.M. respectively along with the postdoctoral grant 740732 for G.M.A. The Spanish government grant (PGC2018-095953-I100) is also gratefully acknowledged.

Acknowledgement

We acknowledge the instrumental support of the Unit for Support to Research and Industry (USAII) at the School of Chemistry at UNAM. We also acknowledge experimental advice of Hugo Hernández-Toledo. The authors also thank DGTIC/UNAM project LANCAD-DGTIC-UNAM-

250 for computer time. G. Moreno-Alcántar wishes to thank Prof. Luisa De Cola for helpful discussions.

ABBREVIATIONS

QTAIM, Quantum Theory of Atoms in Molecules; NCI, Non-Covalent Interactions; Ph, Phenyl, BCP, Bond Critical Point; TMS, Tetramethylsilane; DI, Delocalization Index.

REFERENCES

- (1) Lehn, J.-M. *Supramolecular Chemistry*; Wiley, 1995. <https://doi.org/10.1002/3527607439>.
- (2) Ai, P.; Mauro, M.; De Cola, L.; Danopoulos, A. A.; Braunstein, P. A Bis(Diphosphanil N-Heterocyclic Carbene) Gold Complex: A Synthone for Luminescent Rigid AuAg₂ Arrays and Au₅ and Cu₆ Double Arrays. *Angew. Chemie Int. Ed.* **2016**, *55* (10), 3338–3341. <https://doi.org/10.1002/anie.201510150>.
- (3) Vallejo, J.; Fortea-Pérez, F. R.; Pardo, E.; Benmansour, S.; Castro, I.; Krzystek, J.; Armentano, D.; Cano, J. Guest-Dependent Single-Ion Magnet Behaviour in a Cobalt(II) Metal–Organic Framework. *Chem. Sci.* **2016**, *7* (3), 2286–2293. <https://doi.org/10.1039/C5SC04461H>.
- (4) Yam, V. W.-W.; Au, V. K.-M.; Leung, S. Y.-L. Light-Emitting Self-Assembled Materials Based on d⁸ and d¹⁰ Transition Metal Complexes. *Chem. Rev.* **2015**, *115* (15), 7589–7728. <https://doi.org/10.1021/acs.chemrev.5b00074>.
- (5) Córdón, J.; Jiménez-Osés, G.; López-de-Luzuriaga, J. M.; Monge, M. The Key Role of Au-Substrate Interactions in Catalytic Gold Subnanoclusters. *Nat. Commun.* **2017**, *8* (1), 1657. <https://doi.org/10.1038/s41467-017-01675-1>.

- (6) Davis, H. J.; Phipps, R. J. Harnessing Non-Covalent Interactions to Exert Control over Regioselectivity and Site-Selectivity in Catalytic Reactions. *Chem. Sci.* **2017**, *8* (2), 864–877. <https://doi.org/10.1039/C6SC04157D>.
- (7) Tiekink, E. R. T. Supramolecular Assembly Based on “Emerging” Intermolecular Interactions of Particular Interest to Coordination Chemists. *Coord. Chem. Rev.* **2017**, *345*, 209–228. <https://doi.org/10.1016/j.ccr.2017.01.009>.
- (8) Aliprandi, A.; Mauro, M.; De Cola, L. Controlling and Imaging Biomimetic Self-Assembly. *Nat. Chem.* **2016**, *8* (1), 10–15. <https://doi.org/10.1038/nchem.2383>.
- (9) Molčanov, K.; Kojić-Prodić, B.; Raos, N. Analysis of the Less Common Hydrogen Bonds Involving Ester Oxygen sp^3 Atoms as Acceptors in the Crystal Structures of Small Organic Molecules. *Acta Crystallogr. Sect. B Struct. Sci.* **2004**, *60* (4), 424–432. <https://doi.org/10.1107/S0108768104014442>.
- (10) Novikov, A. S.; Ivanov, D. M.; Bikbaeva, Z. M.; Bokach, N. A.; Kukushkin, V. Y. Noncovalent Interactions Involving Iodofluorobenzenes: The Interplay of Halogen Bonding and Weak $LP(O) \cdots \pi$ -Hole Arene Interactions. *Cryst. Growth Des.* **2018**, *18* (12), 7641–7654. <https://doi.org/10.1021/acs.cgd.8b01457>.
- (11) Grimme, S. Supramolecular Binding Thermodynamics by Dispersion-Corrected Density Functional Theory. *Chem. - A Eur. J.* **2012**, *18* (32), 9955–9964. <https://doi.org/10.1002/chem.201200497>.
- (12) Schottel, B. L.; Chifotides, H. T.; Dunbar, K. R. Anion- π Interactions. *Chem. Soc. Rev.* **2008**, *37* (1), 68–83. <https://doi.org/10.1039/B614208G>.

- (13) Fujii, A.; Shibasaki, K.; Kazama, T.; Itaya, R.; Mikami, N.; Tsuzuki, S. Experimental and Theoretical Determination of the Accurate Interaction Energies in Benzene–Halomethane: The Unique Nature of the Activated CH/ π Interaction of Haloalkanes. *Phys. Chem. Chem. Phys.* **2008**, *10* (19), 2836. <https://doi.org/10.1039/b717053j>.
- (14) Mirzaei, M.; Eshtiagh-Hosseini, H.; Bauzá, A.; Zarghami, S.; Ballester, P.; Mague, J. T.; Frontera, A. On the Importance of Non Covalent Interactions in the Structure of Coordination Cu(II) and Co(II) Complexes of Pyrazine- and Pyridine-Dicarboxylic Acid Derivatives: Experimental and Theoretical Views. *CrystEngComm* **2014**, *16* (27), 6149–6158. <https://doi.org/10.1039/C4CE00003J>.
- (15) Otero-de-la-Roza, A.; Mallory, J. D.; Johnson, E. R. Metallophilic Interactions from Dispersion-Corrected Density-Functional Theory. *J. Chem. Phys.* **2014**, *140* (18), 18A504. <https://doi.org/10.1063/1.4862896>.
- (16) Sadhu, B.; Sundararajan, M.; Bandyopadhyay, T. Efficient Separation of Europium Over Americium Using Cucurbit-[5]-Uril Supramolecule: A Relativistic DFT Based Investigation. *Inorg. Chem.* **2016**, *55* (2), 598–609. <https://doi.org/10.1021/acs.inorgchem.5b01627>.
- (17) Ulloa, C. O.; Ponce-Vargas, M.; Muñoz-Castro, A. Formation of Coinage-Metal···Fullerene Adducts. Evaluation of the Interaction Nature between Triangular Coinage Metal Complexes ($M_3 = \text{Cu, Ag, and Au}$) and C_{60} through Relativistic Density Functional Theory Calculations. *J. Phys. Chem. C* **2018**, *122* (43), 25110–25117. <https://doi.org/10.1021/acs.jpcc.8b08417>.
- (18) Schmidbaur, H.; Schier, A. Auophilic Interactions as a Subject of Current Research: An

- up-date. *Chem. Soc. Rev.* **2012**, *41* (1), 370–412. <https://doi.org/10.1039/C1CS15182G>.
- (19) Bardají, M.; Teresa de la Cruz, M.; Jones, P. G.; Laguna, A.; Martínez, J.; Dolores Villacampa, M. Luminescent Dinuclear Gold Complexes of Bis(Diphenylphosphano)Acetylene. *Inorganica Chim. Acta* **2005**, *358* (5), 1365–1372. <https://doi.org/10.1016/j.ica.2004.05.017>.
- (20) Schmidbaur, H. Supramolecular Chemistry: Going for Gold. *Nature* **2001**, *413* (6851), 31–33. <https://doi.org/10.1038/35092657>.
- (21) He, X.; Yam, V. W.-W. Luminescent Gold(I) Complexes for Chemosensing. *Coord. Chem. Rev.* **2011**, *255* (17–18), 2111–2123. <https://doi.org/10.1016/j.ccr.2011.02.003>.
- (22) Yam, V. W.-W.; Wong, K. M.-C. Luminescent Metal Complexes of d^6 , d^8 and d^{10} Transition Metal Centres. *Chem. Commun.* **2011**, *47* (42), 11579. <https://doi.org/10.1039/c1cc13767k>.
- (23) Yam, V. W.-W.; Cheng, E. C.-C. Highlights on the Recent Advances in Gold Chemistry a Photophysical Perspective. *Chem. Soc. Rev.* **2008**, *37*, 1806–1813. <https://doi.org/10.1039/b708615f>.
- (24) Blanco, M. C.; Cámara, J.; Gimeno, M. C.; Laguna, A.; James, S. L.; Lagunas, M. C.; Villacampa, M. D. Synthesis of Gold-Silver Luminescent Honeycomb Aggregates by Both Solvent-Based and Solvent-Free Methods. *Angew. Chemie Int. Ed.* **2012**, *51* (39), 9777–9779. <https://doi.org/10.1002/anie.201204859>.
- (25) Blake, A. J.; Donamaría, R.; Lippolis, V.; López-de-Luzuriaga, J. M.; Monge, M.; Olmos, M. E.; Seal, A.; Weinstein, J. A. Unequivocal Experimental Evidence of the Relationship between Emission Energies and Auophilic Interactions. *Inorg. Chem.* **2019**, *58* (8), 4954–

4961. <https://doi.org/10.1021/acs.inorgchem.8b03621>.
- (26) England, K. R.; Lim, S. H.; Luong, L. M. C.; Olmstead, M. M.; Balch, A. L. Vapoluminescent Behavior and the Single-Crystal-to-Single-Crystal Transformations of Chloroform Solvates of $[\text{Au}_2(\mu\text{-}1,2\text{-bis}(\text{diphenylarsino})\text{ethane})_2](\text{AsF}_6)_2$. *Chem. – A Eur. J.* **2019**, *25* (3), 874–878. <https://doi.org/10.1002/chem.201804937>.
- (27) Wu, M.; Zhao, J.; Chevrier, D. M.; Zhang, P.; Liu, L. Luminescent Au(I)–Thiolate Complexes through Aggregation-Induced Emission: The Effect of pH during and Post Synthesis. *J. Phys. Chem. C* **2019**, *123* (10), 6010–6017. <https://doi.org/10.1021/acs.jpcc.8b11716>.
- (28) Ghimire, M. M.; Nesterov, V. N.; Omary, M. A. Remarkable Auophilicity and Photoluminescence Thermochromism in a Homoleptic Cyclic Trinuclear Gold(I) Imidazolate Complex. *Inorg. Chem.* **2017**, *56* (20), 12086–12089. <https://doi.org/10.1021/acs.inorgchem.7b01679>.
- (29) Schmidbaur, H.; Schier, A. A Briefing on Auophilicity. *Chem. Soc. Rev.* **2008**, *37* (9), 1931–1951. <https://doi.org/10.1039/b708845k>.
- (30) Muñiz, J.; Wang, C.; Pyykkö, P. Auophilicity: The Effect of the Neutral Ligand L on $[\{\text{ClAuL}\}_2]$ Systems. *Chem. – A Eur. J.* **2011**, *17* (1), 368–377. <https://doi.org/10.1002/chem.201001765>.
- (31) Pyykkö, P.; Zhao, Y. Ab Initio Calculations on the $(\text{ClAuPH}_3)_2$ Dimer with Relativistic Pseudopotential: Is the “Auophilic Attraction” a Correlation Effect? *Angew. Chemie Int. Ed. English* **1991**, *30* (5), 604–605. <https://doi.org/10.1002/anie.199106041>.

- (32) Moreno-Alcántar, G.; Guevara-Vela, J. M.; Delgadillo-Ruíz, R.; Rocha-Rinza, T.; Martín Pendás, Á.; Flores-Álamo, M.; Torrens, H. Structural Effects of Trifluoromethylation and Fluorination in Gold(I) BIPHEP Fluorothiolates. *New J. Chem.* **2017**, *41* (19), 10537–10541. <https://doi.org/10.1039/C7NJ02202F>.
- (33) Brands, M. B.; Nitsch, J.; Guerra, C. F. Relevance of Orbital Interactions and Pauli Repulsion in the Metal–Metal Bond of Coinage Metals. *Inorg. Chem.* **2018**, *57* (5), 2603–2608. <https://doi.org/10.1021/acs.inorgchem.7b02994>.
- (34) Jiang, Y.; Alvarez, S.; Hoffmann, R. Binuclear and Polymeric Gold(I) Complexes. *Inorg. Chem.* **1985**, *24* (1), 749–757. <https://doi.org/10.1021/ic00199a023>.
- (35) Laguna, A. *Modern Supramolecular Gold Chemistry*; Laguna, A., Ed.; Wiley-VCH Verlag GmbH & Co. KGaA: Weinheim, Germany, 2008. <https://doi.org/10.1002/9783527623778>.
- (36) Blasco, D.; López-de-Luzuriaga, J. M.; Monge, M.; Olmos, M. E.; Pascual, D.; Rodríguez-Castillo, M. Cooperative Au(I)···Au(I) Interactions and Hydrogen Bonding as Origin of a Luminescent Adeninate Hydrogel Formed by Ultrathin Molecular Nanowires. *Inorg. Chem.* **2018**, *57* (7), 3805–3817. <https://doi.org/10.1021/acs.inorgchem.7b03131>.
- (37) Tiekink, E. R. T. Supramolecular Assembly of Molecular Gold(I) Compounds: An Evaluation of the Competition and Complementarity between Auophilic (Au···Au) and Conventional Hydrogen Bonding Interactions. *Coord. Chem. Rev.* **2014**, *275* (I), 130–153. <https://doi.org/10.1016/j.ccr.2014.04.029>.
- (38) Dem'yanov, P. I.; Polestshuk, P. M.; Kostin, V. V. The Nature of Metal-Metal Interactions in Dimeric Hydrides and Halides of Group 11 Elements in the Light of High Level

- Relativistic Calculations. *Chem. - A Eur. J.* **2017**, *23* (14), 3257–3261.
<https://doi.org/10.1002/chem.201605519>.
- (39) Zheng, Q.; Borsley, S.; Nichol, G. S.; Duarte, F.; Cockroft, S. L. The Energetic Significance of Metallophilic Interactions. *Angew. Chemie Int. Ed.* **2019**.
<https://doi.org/10.1002/anie.201904207>.
- (40) Andris, E.; Andrikopoulos, P. C.; Schulz, J.; Turek, J.; Růžička, A.; Roithová, J.; Rulíšek, L. Aurophilic Interactions in [(L)AuCl]⋯[(L')AuCl] Dimers: Calibration by Experiment and Theory. *J. Am. Chem. Soc.* **2018**, *140* (6), 2316–2325.
<https://doi.org/10.1021/jacs.7b12509>.
- (41) Bader, R. F. W. *Atoms in Molecules : A Quantum Theory*; Clarendon Press, 1990.
- (42) Johnson, E. R.; Keinan, S.; Mori-Sánchez, P.; Contreras-García, J.; Cohen, A. J.; Yang, W. Revealing Noncovalent Interactions. *J. Am. Chem. Soc.* **2010**, *132* (18), 6498–6506.
<https://doi.org/10.1021/ja100936w>.
- (43) Moreno-Alcántar, G.; Hess, K.; Guevara-Vela, J. M.; Rocha-Rinza, T.; Martín Pendás, Á.; Flores-Álamo, M.; Torrens, H. π -Backbonding and Non-Covalent Interactions in the JohnPhos and Polyfluorothiolate Complexes of Gold(I). *Dalt. Trans.* **2017**, *46* (37), 12456–12465. <https://doi.org/10.1039/C7DT00961E>.
- (44) Romero-Montalvo, E.; Guevara-Vela, J. M.; Costales, A.; Martín Pendás, Á.; Rocha-Rinza, T. Cooperative and Anticooperative Effects in Resonance Assisted Hydrogen Bonds in Merged Structures of Malondialdehyde. *Phys. Chem. Chem. Phys.* **2017**, *19* (1), 97–107.
<https://doi.org/10.1039/C6CP04877C>.

- (45) Duarte Alaniz, V.; Rocha-Rinza, T.; Cuevas, G. Assessment of Hydrophobic Interactions and Their Contributions through the Analysis of the Methane Dimer. *J. Comput. Chem.* **2015**, *36* (6), 361–375. <https://doi.org/10.1002/jcc.23798>.
- (46) Estévez, L.; Sánchez-Lozano, M.; Mosquera, R. A. Understanding the Electron Density Reorganization upon Stacking vs. H-Bonding Interaction in Methyl Gallate–Caffeine Complexes. *RSC Adv.* **2014**, *4* (48), 25018–25027. <https://doi.org/10.1039/C4RA04028G>.
- (47) Watase, S.; Kitamura, T.; Kanehisa, N.; Shizuma, M.; Nakamoto, M.; Kai, Y.; Yanagida, S. Aggregation through the Quadrupole Interactions of Gold(I) Complex with Triphenylphosphine and Pentafluorobenzenethiolate. *Chem. Lett.* **2003**, *32* (11), 1070–1071. <https://doi.org/10.1246/cl.2003.1070>.
- (48) Watase, S.; Kitamura, T.; Kanehisa, N.; Nakamoto, M.; Kai, Y.; Yanagida, S. A Quadrupole–Quadrupole Stacking Synthron in (2,3,5,6-Tetrafluorobenzenethiolato- κ S)(Triphenylphosphine- κ P)Gold(I). *Acta Crystallogr. Sect. C Cryst. Struct. Commun.* **2004**, *60* (3), m104–m106. <https://doi.org/10.1107/S010827010400157X>.
- (49) Berger, R.; Resnati, G.; Metrangolo, P.; Weber, E.; Hulliger, J. Organic Fluorine Compounds: A Great Opportunity for Enhanced Materials Properties. *Chem. Soc. Rev.* **2011**, *40* (7), 3496–3508. <https://doi.org/10.1039/c0cs00221f>.
- (50) Pérez-Casas, S.; Hernández-Trujillo, J.; Costas, M. Experimental and Theoretical Study of Aromatic–Aromatic Interactions. Association Enthalpies and Central and Distributed Multipole Electric Moments Analysis. *J. Phys. Chem. B* **2003**, *107* (17), 4167–4174. <https://doi.org/10.1021/jp0225828>.

- (51) Bacchi, S.; Benaglia, M.; Cozzi, F.; Demartin, F.; Filippini, G.; Gavezzotti, A. X-Ray Diffraction and Theoretical Studies for the Quantitative Assessment of Intermolecular Arene–Perfluoroarene Stacking Interactions. *Chem. - A Eur. J.* **2006**, *12* (13), 3538–3546. <https://doi.org/10.1002/chem.200501248>.
- (52) Cozzi, F.; Bacchi, S.; Filippini, G.; Pilati, T.; Gavezzotti, A. Competition between Hydrogen Bonding and Arene–Perfluoroarene Stacking. X-Ray Diffraction and Molecular Simulation on 5,6,7,8-Tetrafluoro-2-Naphthoic Acid and 5,6,7,8-Tetrafluoro-2-Naphthamide Crystals. *CrystEngComm* **2009**, *11* (6), 1122–1127. <https://doi.org/10.1039/b820791g>.
- (53) Nishio, M.; Hirota, M.; Umezawa, Y. *The CH-[π] Interaction: Evidence, Nature, and Consequences*; Wiley, 1998.
- (54) Thalladi, V. R.; Weiss, H.-C.; Bläser, D.; Boese, R.; Nangia, A.; Desiraju, G. R. C–H \cdots F Interactions in the Crystal Structures of Some Fluorobenzenes. *J. Am. Chem. Soc.* **1998**, *120* (34), 8702–8710. <https://doi.org/10.1021/ja981198e>.
- (55) Dalvit, C.; Invernizzi, C.; Vulpetti, A. Fluorine as a Hydrogen-Bond Acceptor: Experimental Evidence and Computational Calculations. *Chem. - A Eur. J.* **2014**, *20* (35), 11058–11068. <https://doi.org/10.1002/chem.201402858>.
- (56) Due to Its Similarity with Compounds **11** and **12**, We Analysed the Structures of Related Compounds in Reference 23. The Results Are Available in the ESI.
- (57) Guevara-Vela, J. M.; Chávez-Calvillo, R.; García-Revilla, M.; Hernández-Trujillo, J.; Christiansen, O.; Francisco, E.; Martín Pendás, Á.; Rocha-Rinza, T. Hydrogen-Bond

- Cooperative Effects in Small Cyclic Water Clusters as Revealed by the Interacting Quantum Atoms Approach. *Chem. - A Eur. J.* **2013**, *19* (42), 14304–14315. <https://doi.org/10.1002/chem.201300656>.
- (58) Szymczak, J. J.; Grabowski, S. J.; Roszak, S.; Leszczynski, J. H $\cdots\sigma$ Interactions - An Ab Initio and “atoms in Molecules” Study. *Chem. Phys. Lett.* **2004**, *393* (1–3), 81–86. <https://doi.org/10.1016/j.cplett.2004.05.123>.
- (59) Macchi, P.; Sironi, A. Chemical Bonding in Transition Metal Carbonyl Clusters: Complementary Analysis of Theoretical and Experimental Electron Densities. *Coord. Chem. Rev.* **2003**, *238*, 383–412. [https://doi.org/10.1016/S0010-8545\(02\)00252-7](https://doi.org/10.1016/S0010-8545(02)00252-7).
- (60) Fackler, J. P.; Staples, R. J.; Elduque, A.; Grant, T.; Fackler Jnr, J. P.; Staples, R. J.; Elduque, A.; Grant, T. Benzenethiolato(Triphenylphosphine)Gold(I). *Acta Crystallogr. Sect. C Cryst. Struct. Commun.* **1994**, *50* (4), 520–523. <https://doi.org/10.1107/S0108270193009254>.
- (61) Moreno-Alcántar, G.; Salazar, L.; Romo-Islas, G.; Flores-Álamo, M.; Torrens, H. Exploring the Self-Assembled Tacticity in Auophilic Polymeric Arrangements of Diphosphanegold(I) Fluorothiolates. *Molecules* **2019**, *24* (23), 4422. <https://doi.org/10.3390/molecules24234422>.
- (62) Emeléus, H. J.; MacDuffie, D. E. Notes. *J. Chem. Soc.* **1961**, *0* (0), 2572–2600. <https://doi.org/10.1039/JR9610002572>.
- (63) Fackler Jr., J. P.; Douglas, B. E.; Holt Jr., S. L.; Worrell, J. H.; Grimes, R. N.; Angelici, R. *J. Inorganic Syntheses*; Ginsberg, A. P., Ed.; Inorganic Syntheses; John Wiley & Sons, Inc.:

Hoboken, NJ, USA, 1990; Vol. 27. <https://doi.org/10.1002/9780470132586>.

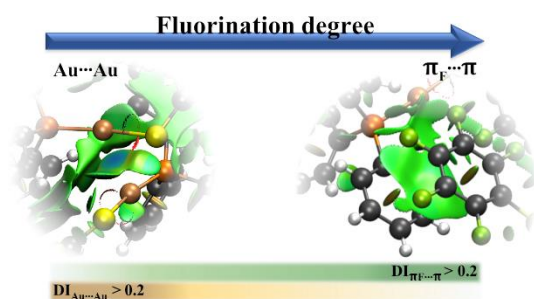
- (64) Delgado, E.; Hernandez, E. Gold(I) Complexes with Thiolate and Triphenylphosphine Ligands. *Polyhedron* **1992**, *11* (24), 3135–3138. [https://doi.org/10.1016/S0277-5387\(00\)83654-2](https://doi.org/10.1016/S0277-5387(00)83654-2).
- (65) Moreno-Alcántar, G.; Hernández-Toledo, H.; Guevara-Vela, J. M.; Rocha-Rinza, T.; Martín Pendás, Á.; Flores-Álamo, M.; Torrens, H. Stability and Trans Influence in Fluorinated Gold(I) Coordination Compounds. *Eur. J. Inorg. Chem.* **2018**, *2018* (40), 4413–4420. <https://doi.org/10.1002/ejic.201800567>.
- (66) Neese, F. The ORCA Program System. *Wiley Interdiscip. Rev. Comput. Mol. Sci.* **2012**, *2* (1), 73–78. <https://doi.org/10.1002/wcms.81>.
- (67) Levy, M.; Perdew, J. P. Success of Quantum Mechanical Approximations for Molecular Geometries and Electron–Nuclear Attraction Expectation Values: Gift of the Coulomb Potential? *J. Chem. Phys.* **1986**, *84* (8), 4519–4523. <https://doi.org/10.1063/1.450024>.
- (68) Becke, A. D. Density-Functional Exchange-Energy Approximation with Correct Asymptotic Behavior. *Phys. Rev. A* **1988**, *38* (6), 3098–3100. <https://doi.org/10.1103/PhysRevA.38.3098>.
- (69) Pantazis, D. A.; Chen, X.-Y.; Landis, C. R.; Neese, F. All-Electron Scalar Relativistic Basis Sets for Third-Row Transition Metal Atoms. *J. Chem. Theory Comput.* **2008**, *4* (6), 908–919. <https://doi.org/10.1021/ct800047t>.
- (70) Lenthe, E. Van; Baerends, E. J.; Snijders, J. G. Relativistic Regular Two-component Hamiltonians. *J. Chem. Phys.* **1993**, *99* (6), 4597–4610. <https://doi.org/10.1063/1.466059>.

- (71) van Wüllen, C. Molecular Density Functional Calculations in the Regular Relativistic Approximation: Method, Application to Coinage Metal Diatomics, Hydrides, Fluorides and Chlorides, and Comparison with First-Order Relativistic Calculations. *J. Chem. Phys.* **1998**, *109* (2), 392–399. <https://doi.org/10.1063/1.476576>.
- (72) Bader, R. F. W. Atoms in Molecules. *Acc. Chem. Res.* **1985**, *18*, 9–15. <https://doi.org/10.1002/prot.10414>.
- (73) Matta, C. F.; Boyd, R. J.; Wiley InterScience (Online service). *The Quantum Theory of Atoms in Molecules: From Solid State to DNA and Drug Design*; Wiley-VCH, 2007.
- (74) Farrugia, L. J.; Evans, C.; Lentz, D.; Roemer, M. The QTAIM Approach to Chemical Bonding Between Transition Metals and Carbocyclic Rings: A Combined Experimental and Theoretical Study of $(\eta^5\text{-C}_5\text{H}_5)\text{Mn}(\text{CO})_3$, $(\eta^6\text{-C}_6\text{H}_6)\text{Cr}(\text{CO})_3$, and $(\text{E})\text{-}\{(\eta^5\text{-C}_5\text{H}_4)\text{CF}=\text{CF}(\eta^5\text{-C}_5\text{H}_4)\}(\eta^5\text{-C}_5\text{H}_5)_2\text{Fe}_2$. *J. Am. Chem. Soc.* **2009**, *131* (3), 1251–1268. <https://doi.org/10.1021/ja808303j>.
- (75) Keith, T. A. AIMAll. TK Gristmill Software: Overland Park KS, USA 2016, p AIMAll (version 12.06.03) 2016.
- (76) Contreras-García, J.; Johnson, E. R.; Keinan, S.; Chaudret, R.; Piquemal, J. P.; Beratan, D. N.; Yang, W. NCIPLLOT: A Program for Plotting Noncovalent Interaction Regions. *J. Chem. Theory Comput.* **2011**, *7* (3), 625–632. <https://doi.org/10.1021/ct100641a>.
- (77) Humphrey, W.; Dalke, A.; Schulten, K. VMD: Visual Molecular Dynamics. *J. Mol. Graph.* **1996**, *14* (1), 33–38. [https://doi.org/10.1016/0263-7855\(96\)00018-5](https://doi.org/10.1016/0263-7855(96)00018-5).
- (78) Agilent Technologies. CrysAlis PRO and CrysAlis RED. Agilent Technologies: Yarnton,

England 2013.

- (79) Clark, R. C.; Reid, J. S. The Analytical Calculation of Absorption in Multifaceted Crystals. *Acta Crystallogr. Sect. A Found. Crystallogr.* **1995**, *51* (6), 887–897. <https://doi.org/10.1107/S0108767395007367>.
- (80) Sheldrick, G. M. Crystal Structure Refinement with SHELXL. *Acta Crystallogr. Sect. C Struct. Chem.* **2015**, *71* (1), 3–8. <https://doi.org/10.1107/S2053229614024218>.
- (81) Sheldrick, G. M. SHELXT – Integrated Space-Group and Crystal-Structure Determination. *Acta Crystallogr. Sect. A Found. Adv.* **2015**, *71* (1), 3–8. <https://doi.org/10.1107/S2053273314026370>.
- (82) Farrugia, L. J. WinGX and ORTEP for Windows: An Update. *J. Appl. Crystallogr.* **2012**, *45* (4), 849–854. <https://doi.org/10.1107/S0021889812029111>.

For Table of Contents Only



We analyze the supramolecular interactions directing the crystalline packing of gold(I) compounds using the NCI-index and QTAIM theoretical methods. Our results reveal the effects of ligand fluorination in the prevalence of different supramolecular interactions: aurophilic contacts, hydrogen bonds and π -stacking.